

Calibration features of a polarimetric back-scattering setup with a beamsplitter

V. Stefanov, B.P. Singh and A. Stefanov

*Institute of Applied Physics, University of Bern,
Sidlerstrasse 5, CH-3012 Bern, Switzerland*

arXiv:2502.10763v1 [physics.optics] 15 Feb 2025

Abstract

We consider the problem of calibrating a polarimetric back-scattering setup with a beamsplitter, taking into account its optical properties. We justify, via Fisher information, a special calibration configuration of reference optical elements for the maximum likelihood method and demonstrate its effectiveness numerically through Monte Carlo simulations. Additionally, we highlight the importance of considering the beamsplitter's optical properties by proposing a test to estimate the error resulting from neglecting these properties during the calibration procedure.

I. INTRODUCTION

Polarimetry is a strong experimental tool for characterizing the optical properties of objects of interest. It finds numerous applications in biomedical applications [1, 2], astronomy [3, 4], geology [5] and more [6]. The distinctly different polarization features of an object's components provide excellent contrast and high sensitivity. Nowadays, polarimetry-based devices represent one of the most promising directions for recognizing various types of cancer in vivo or during surgical procedures [7–9].

The full polarimetric properties of samples can be probed either in transmission or in reflection. The usual reflection configuration is only sensitive to the surface of the sample [10–12]. Here we are focusing on the so-called back-scattering configuration [13, 14], that enables the study of the internal scattering properties of a sample rather than just its surface, making it useful for cases beyond histological analysis [?]. A set of points with equal polarimetric properties can delineate the border between parts with different internal structures, such as the boundary between anisotropic brain tissue and tumors [15]. Together with time-resolving detection this method potentially allows a tissue sample to be studied layer by layer to the full penetration depth [16]. The back-scattering setup uses a focused illumination, implying a short working distance. Therefore, is usually separate the illumination light from the collected back-scattered light by a beamsplitter (BS).

The technical essence of polarimetry is in defining the so-called Mueller matrix of each point of the studied object. The Mueller matrix is a 4×4 table that contains complete information about polarization properties, enabling the prediction of all possible polarizations of scattered light at the given point.

The definition of a Mueller matrix requires conducting at least 16 measurements for

each pair from the four possible input and output polarizations (they are generated by a polarization state generator PSG and a polarization state analyzer PSA respectively). Our knowledge of the values of PSG and PSA is one of the factors determining the setup's accuracy. There are several calibration methods available to measure them, such as the eigenvalue calibration methods (ECM) [17–19], the maximum likelihood calibration method (MLCM) [20], and others [21, 22], but most of them are hardly suitable for a back-scattering polarimetric setup. The reason is the presence of a BS and the necessity of taking into account its optical properties. In this paper we show a configuration of reference elements that allows to calibrate setup directly via MLCM without additional manipulation of the BS.

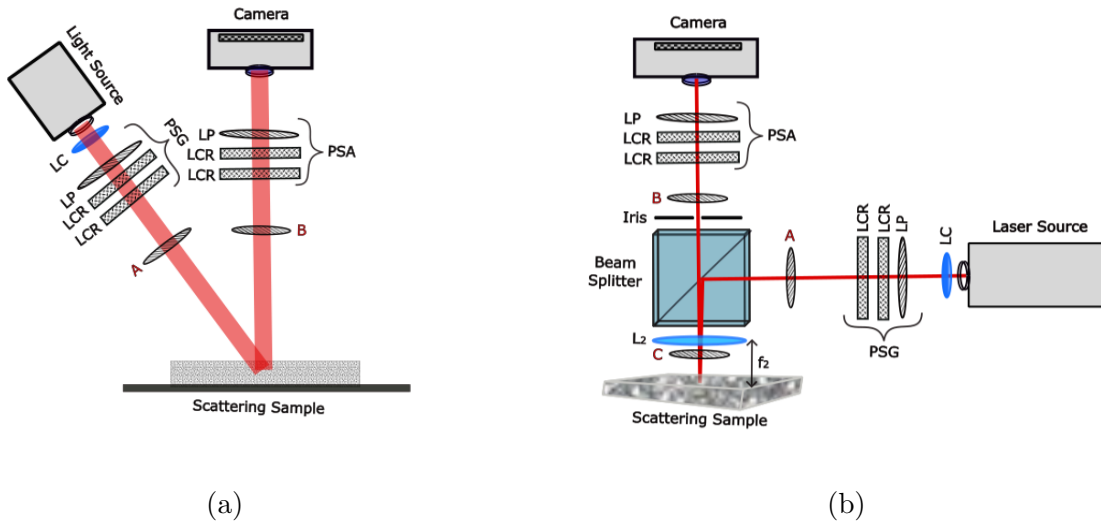


Figure 1. Two different principal schemes of a polarimetric back-scattering setup (a) reflective and (b) scanning.

The paper is organized as follows: we first provide a brief review of common calibration methods. Next, we describe a suitable calibration scheme for a BS setup and also explain the features of using various optical elements. Then we suggest a test to estimate errors of different calibration schemes, and, finally, we demonstrate superiority of the suggested scheme through experimental validation, followed by a discussion.

II. COMMON CALIBRATION METHODS

We can collect the Stokes vectors generated by the PSG and PSA in matrices, denoted W and A respectively. This allows us to express the measured intensity values in a matrix I and match the expression $I = AMW$ in configuration without a BS (Type I at Fig.1a) and $I = ATMBW$ in configuration with one (Type II at Fig.1b), where M , B and T are the Mueller matrices of a sample, the reflected and transmitted sides of the BS respectively. A calibration involves retrieving the pair of matrices A and W for Type I or AT and BW for Type II from a set of measurements. For this purpose, either reference optical elements with known Mueller matrices or optical elements with easily reconstructed Mueller matrices are used, such as linear polarizers (P), wave-plates, mirrors or other reflected samples (R).

Below we briefly explain the essence of the eigenvalues calibration method (ECM) [17], and of the maximum likelihood calibration method (MLCM) [20].

A. Eigenvalues Calibration Method

According to the ECM, the four measured intensity matrices: two with reflected samples (AR_1W , AR_2W) and two with a linear polarizer placed after the PSG (AR_1PW) and before the PSA (APR_1W) are enough for calibration. The method based on the fact that the eigenvalues of $W^{-1}R_1W$ are the same as of R_1 . For this reason a calculation of the eigenvalues of the expression $(AR_1W)^{-1}(AR_1PW)$ allows to restore the Mueller matrix of the linear polarizer P without respect of orientation angle θ and the expression $(AR_1W)^{-1}(AR_2W)$ allows to restore the intermediate matrix $R_1^{-1}R_2$. Due to a presence of noise we have to make additional transformation, so we define the matrices $H_1(\theta)$ (as function of θ) and H_2 :

$$H_1(\theta) = E \otimes P(\theta) - [(AR_1W)^{-1}(AR_1PW)]^T \otimes E, \quad (1)$$

$$H_2 = E \otimes R_1^{-1}R_2 - [(AR_1W)^{-1}(AR_2W)]^T \otimes E, \quad (2)$$

where \otimes means tensor product, E is the identity matrix, a Mueller matrix $P(\theta) = J(\theta)PJ(-\theta)$ with the polarizer matrix $P = \tau_p \mathfrak{G}(1, 0, 0)$ and with a rotation matrix $J(\theta)$:

$$\mathfrak{G}(x, y, z) = \frac{1}{2} \begin{bmatrix} 1 & x & 0 & 0 \\ x & 1 & 0 & 0 \\ 0 & 0 & y & z \\ 0 & 0 & -z & y \end{bmatrix}, J(\theta) = \begin{bmatrix} 1 & 0 & 0 & 0 \\ 0 & \cos 2\theta & -\sin 2\theta & 0 \\ 0 & \sin 2\theta & \cos 2\theta & 0 \\ 0 & 0 & 0 & 1 \end{bmatrix}. \quad (3)$$

The Mueller matrices of reflected samples is parametrized by:

$$R_m = R(\tau_m, \psi_m, \Delta_m) \equiv 2\tau_m \mathfrak{G}(-\cos 2\psi_m, \sin 2\psi_m \cos \Delta_m, \sin 2\psi_m \sin \Delta_m), \quad (4)$$

for $m = 1, 2$, where τ is a transmissivity, ψ and Δ are ellipsometric angles.

The linear mapping $K(\theta)$:

$$K(\theta) = H_1(\theta)^T H_1(\theta) + H_2^T H_2, \quad (5)$$

allows to define orientation of the linear polarizer θ by minimizing the ratio of it smallest and second smallest eigenvalues. The eigenvector of $K(\theta)$ corresponding to the smallest eigenvalue must be associated with the estimator of W , written in lexicographic order. The using of set APR_1W , AR_1W and AR_2W allows us to define A in a similar manner.

B. Maximum Likelihood Calibration Method

The another possible way to make calibration of a setup is a maximum likelihood calibration method (MLCM). For a given set of measurements, the MLCM allows to estimate the most likely state [23]. To make calibration via MLCM we need to maximize the likelihood function $\mathfrak{L}(\zeta)$ over the set of all parameters of setup $\{\zeta\}$:

$$\{\zeta\} = \arg \max_{\zeta} \mathfrak{L}(\zeta). \quad (6)$$

Usually it is more convenient to use natural logarithm of the likelihood function, called the log-likelihood $\mathfrak{l}(\zeta) = \log \mathfrak{L}(\zeta)$. The explicit form of the log-likelihood depends on the statistical distribution of the noise we are dealing with. In this paper, we assume to deal with Gaussian sources of noise, and we are writing expressions of the log-likelihood for it:

$$\mathfrak{l}(\zeta) = -\frac{1}{2\sigma^2} \sum_j Tr [(I_j - \beta_j AM_j W) \cdot (I_j - \beta_j AM_j W)^T], \quad (7)$$

where σ represents the standard deviation of Gaussian noise, j denotes the measurement number, β_j stands for the effective transmittance coefficient and M_j is the Mueller matrix correspondent to the measurement j .

Both matrices $A = \{\mathbf{S}_1, \dots, \mathbf{S}_4\}$ and $W^T = \{\mathbf{S}_5, \dots, \mathbf{S}_8\}$ contain four Stokes vectors in standard form $\mathbf{S}_l = \{I_l, Q_l, U_l, V_l\}$. Because during numerical calculation we are not able to distinguish the transmittance input of each j -measurement part in the effective coefficient β , it is logical to normalize A by I_1 and W by I_5 and hide them in β explicitly.

Due to linearity of dependency on β in (7) we can estimate them directly as

$$\frac{\partial \mathfrak{I}}{\partial \beta_j} = 0. \quad (8)$$

Here it is important to distinguish the equal β_j coefficients that are attached to different measurements, for example if we are fitting the data of several different orientations of an one polarizer. Then the expression for maximization can be converted in form:

$$\mathfrak{I}(\zeta) = \sum_s \frac{\left(\sum_{i_s} \text{Tr} [(AM_{i_s} W) \cdot I_{i_s}^T] \right)^2}{\sum_{i_s} \text{Tr} [(AM_{i_s} W) \cdot (AM_{i_s} W)^T]}, \quad (9)$$

where we have s sets of $i_s \geq 1$ measurements with the equal staff, and the effective coefficient β is equal to:

$$\beta_s = \frac{\sum_{i_s} \text{Tr} [(AM_{i_s} W) \cdot I_{i_s}^T]}{\sum_{i_s} \text{Tr} [(AM_{i_s} W) \cdot (AM_{i_s} W)^T]}. \quad (10)$$

III. CALIBRATION CONFIGURATION FOR BACK-SCATTERING SETUP WITH A BEAMSPLITTER

ECM enables the reconstruction of only two generalized Mueller matrices separated by polarizer at the position A and B on Fig. 1b. This poses a challenge for setups involving a BS. Indeed, when calibrating both PSA and PSG together with a BS via ECM, placing the polarizer between the sample and the BS (the position C on Fig. 1b) results in the light passing through the BS twice: first immediately after the BS and then after reflection from the sample. The full Mueller matrix of system can be written as $AP(-\theta)R_1P(\theta)W$. This makes impossible the determination of the H_i matrices (1) and (2), because the main

statement about a possibility of reconstruction $P(\theta)$ (and $R_1^{-1}R_2$) based on the equality of eigenvalues for $W^{-1}P(\theta)W$ and $P(\theta)$ doesn't occur here.

There are some modification of ECM for such kind of configuration, but only if we make some assumptions on the BS and a reference sample. In particular, if a part of the setup between PSG and PSA shows only retardance (and doesn't exhibit depolarisation, diattenuation or polarisation) [24].

However, the MLCM allows to deal with any configuration of the system included the case described above. But to separate the PSG and PSA matrices from a sample, we need to place a reference optical element in position C Fig.1(a). For the calibration with this auxiliary optical elements F set at angles θ_i and with sample M , the total expression for maximizing via MLCM for this configuration has the form (9) with $M_{i_s} = F_s(-\theta_i)MF_s(\theta_i)$, where F_s oriented for θ_i as $F_s(\theta_i) = J(\theta_i)F_sJ(-\theta_i)$.

An important feature of the MLCM is that it may not exhibit high sensitivity to variations of variables in case of its small impact. This means that it can still produce reasonable calibration values, even in cases where the set of measurements is poorly defined. In fact, MLCM can find a solution even when some variables are almost indistinguishable within the measurement set, due to the influence of initial conditions and noise in the intensity measurements. To mitigate this issue, it is essential to estimate the errors associated with the calibration parameters. One effective way to achieve this is by using the Fisher Information (FI) apparatus [25], which helps quantify the uncertainty of restoring variables in dependence on an experimental noise.

A. Fisher information

The Fisher information measures the overall sensitivity of the functional relationship $f(x|\mu)$ to changes of μ by weighting the sensitivity at each potential outcome x with respect to the chance defined by $p_\mu(x) = f(x|\mu)$ [26], and can be expressed in form:

$$\mathfrak{F}(\mu)_{nm} = \int_M dx \left(\frac{\partial}{\partial \mu_n} \log f(x|\mu) \right) \left(\frac{\partial}{\partial \mu_m} \log f(x|\mu) \right) p_\mu(x). \quad (11)$$

For continuous set of 30 variables[27] $\mu = \{\mu_A, \mu_W\}$, where $\mu_A = \{\mathbf{S}_i\}$ (explicit form is $\mu_A = \{Q_1, U_1, V_1, I_2, Q_2, \dots, I_4, Q_4, U_4, V_4\}$) and $\mu_W = \{\mathbf{S}_{4+i}\}$ (explicit form is $\mu_W = \{Q_5, U_5, V_5, I_6, Q_6, \dots, I_8, Q_8, U_8, V_8\}$) for $i = \overline{1,4}$ without I_1 and I_5 . We can suggest for

each particular measurement, that intensity is normally-distributed (with variance σ^2) and doesn't depend on others. Also we can suggest the identity of their variance regardless of an intensity value. Then the FI simplifies[28]:

$$\mathfrak{F}_{nm} = \frac{1}{\sigma^2} \sum_{k,l,F,i} \frac{\partial}{\partial \mu_n} \left((\tilde{A}F(-\theta_i)MF(\theta_i)\tilde{W})_{kl} \right) \frac{\partial}{\partial \mu_m} \left((\tilde{A}F(-\theta_i)MF(\theta_i)\tilde{W})_{kl} \right). \quad (12)$$

Diagonal elements of an inverse FI shows a lower bound of error on the variance for correspondent variables (also known as the Cramér–Rao bound [28] - CRB):

$$\Delta^2 \mu_n \geq (\mathfrak{F})^{-1}_{nn}. \quad (13)$$

Thus, the existing of the inverse FI means principal possibility of restoring μ . And moreover, the magnitude of diagonal elements shows us the difference in their error relative to each other. This allows us to supplement the calibration procedure, as we can now study the calibration configuration theoretically, predict and deal with potential issues that may arise from it.

Also we can answer how many measurements do we need for unambiguous restoring of A and W for chosen calibration configuration. It can be done for certain set of measurements by a lot of ways, directly through checking the existing of inverse FI, through calculation eigenvalues of FI (all of them must be non-zero) or a matrix rank of FI.

B. Features of using common optical elements

There are some comments about using a quarter-wave plate, a polarizer and a mirror as tools for calibration. In the case of an ideal mirror as a sample $M = 2\mathfrak{G}(0, -1, 0)$, an ideal quarter-wave plate and polarizer are not sufficient for calibration. Indeed, a measurement with an ideal quarter-wave plate $F_Q = Q = 2\mathfrak{G}(0, 0, 1)$ gives $Q(-\theta)MQ(\theta) = J(2\theta)$. This means physically that we rotate both the generator and the analyzer, and that can not provide an additional information about circular polarization (component V_j) comparable with the measurement without a quarter wave plate ($F_0 = \hat{I} = 2\mathfrak{G}(0, 1, 0)$):

$$I_{F_Q} = I_k I_{4+l} + V_k V_{4+l} + (Q_k Q_{4+l} + U_k U_{4+l}) \cos(4\theta) + (Q_{4+l} U_k - Q_k U_{4+l}) \sin(4\theta), \quad (14)$$

$$I_{F_0} = I_k I_{4+l} + V_k V_{4+l} + Q_k Q_{4+l} + U_k U_{4+l}. \quad (15)$$

There is an important feature of calibration procedure of a setup with a BS. Using of quarter-wave plates does not allow us to operate by V components of Stokes vector as free as we

can do by linear ones. There are always a deviation from ideal QWP and mirror in real experiment, however the error of circular components of polarization will be incredibly large.

Particularly, it can be demonstrated explicitly by calculating the FI for a following set of measurements: $\{F = \hat{I}\}; \{F = P, \theta = 0; \pi/4\}; \{F = Q, \theta = \pi/4\}$ with suggestion about a non-ideality of mirror in form $M = 2\mathfrak{G}(0, \cos \gamma, \sin \gamma), \gamma \approx \pi$. After inverting the FI, the Stokes parameters the variance of V grow up with tending γ to π as

$$\lim_{\gamma \rightarrow \pi} \Delta^2 V \sim \sigma^2 \frac{1}{(\pi - \gamma)^2}, \quad (16)$$

while the variance for I , Q and U stays constant. The similar dependence appears, if we have perfect mirror $M = 2\mathfrak{G}(0, -1, 0)$ and almost perfect QWP with Muller matrix $Q = 2\mathfrak{G}(0, \sin \gamma, \cos \gamma)$:

$$\lim_{\gamma \rightarrow 0} \Delta^2 V \sim \sigma^2 \frac{1}{\gamma^2}. \quad (17)$$

If we measure a big number of angles for polarizer and QWP $\theta_j = 2\pi j/N, j = \overline{0, N-1}$, $N \gg 1$ (that means incretion number of measurements to N) we can reduce errors (16), (17) approximately in N times, and taking into account the small value of σ ($\sigma^2 \approx 10^{-6}$) this is still possible to use QWPs for calibration. However, despite the theoretical feasibility to do so, we observe that the errors associated with different components of A and W vary by several degrees. This variation prevents us from considering this configuration as a standard one for calibration. Therefore, we need to find a way to ensure that the errors for all components of the calibration matrices are of the same order of magnitude.

C. Overcoming the difficulties in V-component defining

Because the using of polarizers between a sample and the BS allows to define the linear components in input and output Stokes vectors and doesn't help with circular ones, it seems logical to perform a measurement, where linear and circular components are swapped. We can achieve that separately for W and A by adding a quarter-wave plate before ($Q_1 = 2J(\Theta_1)\mathfrak{G}(0, 0, 1)J(-\Theta_1)$ positions A on Fig.1b) and after ($Q_2 = 2J(\Theta_2)\mathfrak{G}(0, 0, 1)J(-\Theta_2)$ positions B on Fig.1b) the BS. Then we have to extend calibration variables ζ for ellipsometric angles $\{\psi_t, \Delta_t, \psi_b, \Delta_b\}$ from the Mueller matrix $T = R(1, \Delta_t, \psi_t)$ and $B = R(1, \Delta_b, \psi_b)$ [29], that corresponds to the transmitted and the reflected side of the BS correspondingly. We have following sets of measurements:

- reference measurements without polarizer, but with quarter-wave plates:

$$\{M_1(\Theta_1) = TMBQ_1; M_2(\Theta_2) = Q_2TMB\}, \quad (18)$$

- reference measurement without polarizer and quarter-wave plate:

$$\{M_3 = TMB\}, \quad (19)$$

- measurements with polarizer, but without quarter-wave plates:

$$\{M_4(\theta_{i_p}) = TP(\theta_{i_p})MP(-\theta_{i_p})B\} \quad (20)$$

- measurements with polarizer and quarter-wave plates:

$$\{M_5(\theta_{i_{q1}}) = TP(\theta_{i_{q1}})MP(-\theta_{i_{q1}})BQ_1; M_6(\theta_{i_{q2}}) = Q_2TP(\theta_{i_{q2}})MP(-\theta_{i_{q2}})B\}. \quad (21)$$

We will call this configuration as $Q - P - Q$ and the configuration with QWP and polarizer after a BS (in position C (Fig.1b)) as $-P/Q-$ for brevity.

D. Monte-Carlo simulation

To demonstrate the effectivity of $Q - P - Q$ calibration configuration we compare it result of numerical Monte-Carlo simulation with $-P/Q-$ configuration. We assume white Gaussian noise with a standard deviation σ and define a signal to noise ratio:

$$SNR(\sigma) = 10 \log_{10} \frac{1}{\sigma^2}. \quad (22)$$

The accuracy of calibration procedure can be calculated with help of a root-mean-square error of estimator for $W = [w_{ij}]$ and $A = [a_{ij}]$:

$$RMSE = \sqrt{\left\langle \sum_{ij} (a_{ij} - \mathbf{a}_{ij})^2 \right\rangle + \left\langle \sum_{ij} (w_{ij} - \mathbf{w}_{ij})^2 \right\rangle}, \quad (23)$$

where $W_0 = [\mathbf{w}_{ij}]$ and $A_0 = [\mathbf{a}_{ij}]$ are true values of calibration matrices without noise in tetrahedron form [30] (without coefficient 1/2 to avoid confusion in (22)):

$$W_0 = A_0^T = \begin{pmatrix} 1 & 1 & 1 & 1 \\ \frac{1}{\sqrt{3}} & -\frac{1}{\sqrt{3}} & -\frac{1}{\sqrt{3}} & \frac{1}{\sqrt{3}} \\ \frac{1}{\sqrt{3}} & -\frac{1}{\sqrt{3}} & \frac{1}{\sqrt{3}} & -\frac{1}{\sqrt{3}} \\ \frac{1}{\sqrt{3}} & \frac{1}{\sqrt{3}} & -\frac{1}{\sqrt{3}} & -\frac{1}{\sqrt{3}} \end{pmatrix}. \quad (24)$$

The polarizer is assumed to be modeled as $P = 0.85\mathfrak{G}(0.999, 0.01, 0.01)$, the quarter-wave plate as $Q = 0.95 * 2\mathfrak{G}(0.01, 0.01, 0.999)$, the sample $M = R(1, \arctan(0.99), 0.99\pi)$ and the BS matrices $T = R(1, \arctan(0.99), 0.01\pi)$, $B = R(1, \arctan(0.99), 0.99\pi)$.

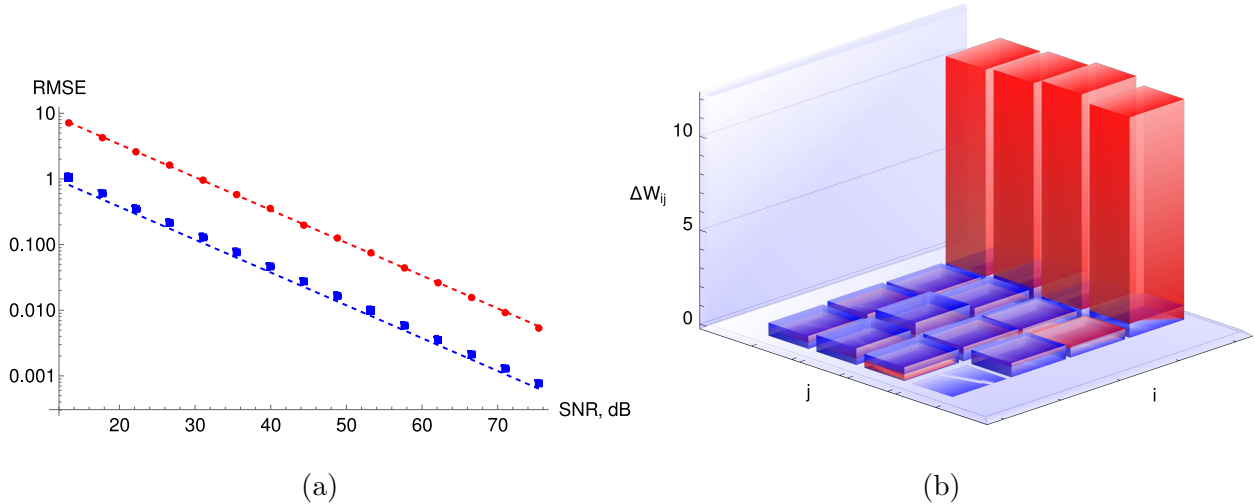


Figure 2. (a) Root mean square error function (23) is in dependence of SNR for two calibration configurations: $Q - P - Q$ (blue points) and $-P/Q-$ (red points). Dashed lines show an analytical expression for minimal error from Cramér–Rao bound. A number of simulation is 1000. (b) Standard deviation for ΔW_{ij} from Cramér–Rao bound is shown for $Q - P - Q$ (blue barchart) and $-P/Q-$ (red barchart).

We simulate 7 measurements for each calibration configurations (results are shown in Fig.2a). For configuration $Q - P - Q$ (blue color) we use measurements $\{M_1(\Theta_1 = \pi/4); M_2(\Theta_2 = \pi/4); M_3; M_4(\theta = 0); M_4(\theta = \pi/4); M_5(\theta = 0, \Theta_1 = \pi/4); M_6(\theta = 0, \Theta_2 = \pi/4)\}$ (blue points), and calculation of the FI (12) gives us $RMSE_{FI} \approx 3.76\sigma$ (blue dashed line). For configuration $-P/Q-$ we take $(\{F = \hat{I}\}; \{F = P, \theta = 0; \pi/9; \pi/4\}; \{F = Q, \theta = 0; \pi/9; \pi/4\})$ (red points) with $RMSE_{FI} \approx 33.66\sigma$ from the FI (12) (red dashed line). In Fig.2b is shown that theoretical error for all components of W has the same order that for configuration (18-21), except circular polarizations as was explained above.

The FI demonstrates correct behavior in Fig.2a, and the difference between theoretical error from (13) and simulations result is a consequence of general sense of the CRB comparing with particular case of restoring parameters thought MLCM.

IV. A TEST FOR DEMONSTRATING THE INFLUENCE OF A BEAMSPLITTER

So, the calibration configuration $Q - P - Q$ allows to recognize both PSG and PSA calibration matrices and moreover the matrices of the BS: T and B . Now it is possible to see what happens in case of ignoring the impact of the BS. We can suggest a test to estimate an error in definition of the orientation of polarizer placed below the BS above the mirror. Without taking into account the impact of the BS the calculated orientation α is consist of the true orientation value θ and systematic error δ . The analytical estimation of systematic error can be calculated from equation $\partial \mathfrak{l}(\alpha)/\partial \alpha = 0$, where $\mathfrak{l}(\alpha)$ has form similar to (9):

$$\mathfrak{l}(\alpha) = \frac{\text{Tr} [(AT^{(id)}P(-\alpha)MP(\alpha)B^{(id)}W) \cdot (AT^{(tr)}P(-\theta)MP(\theta)B^{(tr)}W)^T]^2}{\text{Tr} [(AT^{(id)}P(-\alpha)MP(\alpha)B^{(id)}W) \cdot (AT^{(id)}P(-\alpha)MP(\alpha)B^{(id)}W)^T]}, \quad (25)$$

with ideal BS elements [31, p.483]

$$\begin{aligned} T^{(id)} &= R(1, \pi/4, 0), \\ B^{(id)} &= R(1, \pi/4, \pi), \end{aligned} \quad (26)$$

and with true ones $T^{(tr)} = R(1, \arctan(P_t), \gamma_t)$ and $B^{(tr)} = R(1, \arctan(P_b), \pi - \gamma_b)$.

With following notifications:

$$O = AT^{(id)}P(-\theta)MP(\theta)B^{(id)}W, \quad (27)$$

$$X = \frac{\partial}{\partial \theta} O, \quad (28)$$

$$R = AT^{(tr)}P(-\theta)MP(\theta)B^{(tr)}W - O. \quad (29)$$

we can find a approximate solution for δ from equation $\partial \mathfrak{l}(\alpha)/\partial \alpha = 0$. Indeed, we can restrict ourself by considering only first term in series for δ in (25) because of their smallness. Also, it is possible to simplify solution more if we take into account that that Muller matrices of the real BS is close to ideal ones (R^2 is negligible), and the final solution is

$$\delta^{(approx)} = \frac{\text{Tr} [X \cdot O^T] \text{Tr} [R \cdot O^T] - \text{Tr} [X \cdot R^T] \text{Tr} [O \cdot O^T]}{\text{Tr} [X \cdot O^T]^2 - \text{Tr} [X \cdot X^T] \text{Tr} [O \cdot O^T]}. \quad (30)$$

For Stokes vectors in tetrahedron form (24), the error (30) is equal to

$$\delta^{(tetra)} = \frac{1}{4} ((1 - P_t) + (1 - P_b)) \sin 2\theta - \frac{1}{16} (\gamma_t^2 + \gamma_b^2) \sin 4\theta. \quad (31)$$

For ideal case we have $P_t = P_b = 1$ and $\gamma_t = \gamma_b = 0$, and the error δ disappears.

V. EXPERIMENTAL VALIDATION

We demonstrate the experimental realization of the above test.

The imaging polarimeter utilized in this study is illustrated in Figure 1b. This device shares a common configuration with many polarimeters designed for back-scattering geometry, consisting of two perpendicular arms. The first, horizontally oriented arm is designated for illumination and incorporates the polarization state generator (PSG). The second, vertically oriented arm, used for detection, employs a conventional two-lens system and includes the polarization state analyzer (PSA). The light source is a Picosecond Diode laser LDH-IB-730-B Taiko by PicoQuant, coupled into a single mode fiber, operating at $\lambda = 727.6$ nm. The laser beam generated by the source is collimated using a lens (LC) and directed onto the surface of the system under investigation via a non-polarizing beamsplitter cube (50:50, maintaining polarization within 0.5 % at a $\pi/4$ incidence angle). The PSG, which operates on the collimated beam, is capable of generating any arbitrary polarization state. This component includes a linear polarizer (LP, Nanoparticle Linear Polarizer, Thorlabs, extinction ratio 1 : 100,000) and two computer-controlled liquid crystal variable retarders (LCR, Meadowlark Optics). The fast axis of the first retarder is oriented at $\pi/4$ relative to the x - and y -axes of the laboratory frame, while the fast axis of the second retarder is aligned with the y -axis in the same frame. The polarized illumination beam is subsequently focused onto the sample surface using an objective lens ($L2$) with a focal length of $60mm$. The beam's $1/e^2$ spot radius of $36\mu m$ was ascertained by substituting the scattering system with a customized Pixelink camera for beam profiling and fitting a Gaussian profile to the recorded intensity distribution at various z -positions. The backscattered light traverses a two-lens system comprising the objective lens $L2$ and a second lens $L1$, identical to $L2$. An iris located at the back focal plane of $L2$ determines the numerical aperture (NA) of the imaging instrument. For this study, we employed an NA of 0.066, which is sufficiently small to avoid imaging specular reflections when the illumination beam is slightly tilted ($0.14rad$). The PSA, situated between $L2$ and $L1$, consists of the same components as the PSG, but in reverse order. A CCD chip (ptGray Grasshopper, 16-bit, 2448×2048 pixels) at the end of the detection arm is used to image the backscattered light with a magnification of approximately 1.2. All measurements presented in this study were conducted at $\lambda = 727.6nm$.

If we have the measurement data $I(\theta)$ for configuration mentioned above, then we can try to recognize angle θ for two set of calibration matrices defined via MLMC for $Q - P - Q$ configuration: $A_1 \equiv A \cdot T^{(tr)}$, $W_1 \equiv B^{(tr)} \cdot W$ and $A_2 \equiv A \cdot T^{(id)}$, $W_2 \equiv B^{(id)} \cdot W$ eq. (26). Then, the expression (9) has a new meaning, it is relevant, but for one unknown variable - only the polarizer angle. In Fig. 3 (a) is shown the absolute reconstructed value of angle by two sets of calibration matrices, and in Fig. 3(b) we see the difference between errors in the restoring angle of polarizer (between blue and yellow line in 3(a)). This is a systematic error δ that occurs due to using of unsuitable calibration configuration. Green line in Fig. 3(b) shows the calculation of error δ according the (31), and demonstrate that the suggested approximation is good enough to approximate it.

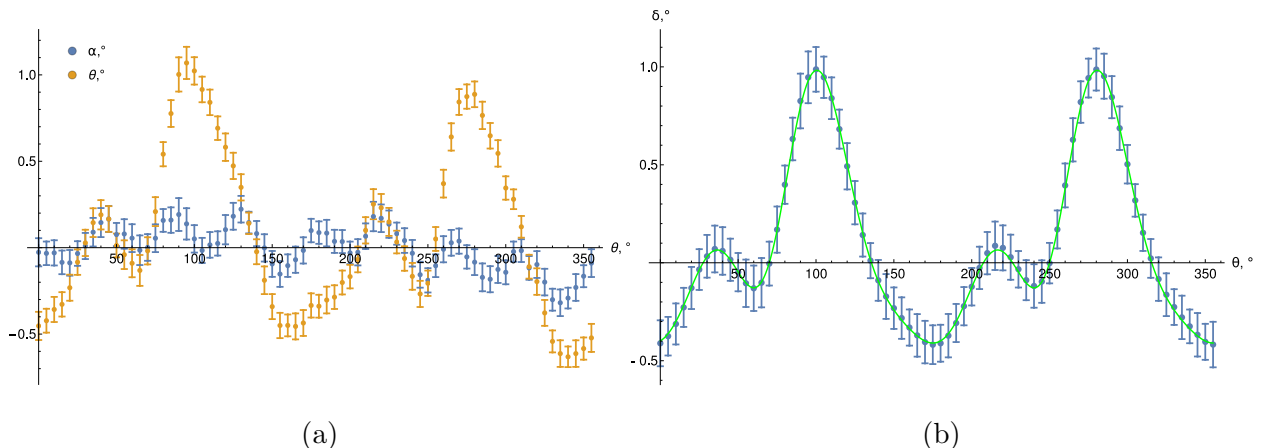


Figure 3. Results of experiment for restoring θ angles. (a) shows errors between restored and true angle for two sets of calibration data, (b) shows the difference of errors (blue dashed line) and fitting plot by expression (30) (green line).

VI. CONCLUSION

In this paper, we demonstrate the importance of a correct calibration method for back-scattering polarization setups using a BS. Obviously, the optical elements of a BS (even those close to ideal) affect the accuracy of measurements. Despite the apparent insignificance of the BS's influence, it cannot be neglected. To account for this, we describe a maximum likelihood calibration method adapted to a setup involving a BS. The so-called $Q - P - Q$ configuration yields errors of the same degree for all components of the calibration matrices,

as shown numerically using the Fisher information framework. Additionally, we present a simple experimental test for restoring the polarizer orientation, which allows us to estimate the error introduced by ignoring the presence of the beamsplitter during the calibration of the setup.

DISCLOSURES

The authors declare no conflicts of interest.

- [1] N. Ghosh and I. A. Vitkin, *Journal of biomedical optics* **16**, 110801 (2011).
- [2] F. T. Ulaby and C. Elachi, *Radar polarimetry for geoscience applications* (Taylor & Francis, 1990).
- [3] K. Serkowski, in *Planets, Stars, and Nebulae: Studied with Photopolarimetry*, *Proceedings of IAU Colloq*, Vol. 23 (1974) p. 135.
- [4] J. Hough, *Journal of Quantitative Spectroscopy and Radiative Transfer* **106**, 122 (2007).
- [5] W. Egan, *Optical Remote Sensing: Science and Technology*, Optical Science and Engineering Series (CRC Press, 2003).
- [6] C. Schmullius and D. L. Evans, *International Journal of Remote Sensing* **18**, 2713 (1997).
- [7] S. N. Tukimin, S. B. Karman, M. Y. Ahmad, and W. S. Wan Kamarul Zaman, *IEEE Sensors Journal* **19**, 9010 (2019).
- [8] D. C. Louie, L. Tchvialeva, S. Kalia, H. Lui, and T. K. Lee, *Journal of biomedical optics* **26**, 035001 (2021).
- [9] J. Qi and D. S. Elson, *Journal of biophotonics* **10**, 950 (2017).
- [10] A. Vitkin, N. Ghosh, and A. d. Martino, *Photonics: Biomedical Photonics, Spectroscopy, and Microscopy*, 239 (2015).
- [11] X. Li, Y. Han, H. Wang, T. Liu, S.-C. Chen, and H. Hu, *Frontiers in physics* **10**, 815296 (2022).
- [12] Y. Guo, N. Zeng, H. He, T. Yun, E. Du, R. Liao, Y. He, and H. Ma, *Optics express* **21**, 18361 (2013).
- [13] A. Jain, A. K. Maurya, L. Ulrich, M. Jaeger, R. M. Rossi, A. Neels, P. Schucht, A. Dommann, M. Frenz, and H. G. Akarçay, *Opt. Express* **28**, 16673 (2020).

- [14] O. Arteaga, E. Garcia-Caurel, and R. Ossikovski, *Optics Letters* **39**, 6050 (2014).
- [15] O. Rodríguez-Núñez and T. Novikova, *Advanced Optical Technologies* **11**, 157 (2022).
- [16] A. Stefanov, P. Tijlkorte, G. Hannink, L. Roth, and M. Frenz, *Opt. Lett.* **48**, 6396 (2023).
- [17] E. Compain, S. Poirier, and B. Drevillon, *Applied optics* **38**, 3490 (1999).
- [18] A. De Martino, E. Garcia-Caurel, B. Laude, and B. Dré villon, *Thin Solid Films* **455**, 112 (2004).
- [19] C. Macias-Romero and P. Török, *Journal of the European Optical Society-Rapid publications* **7** (2012).
- [20] H. Hu, E. Garcia-Caurel, G. Anna, and F. Goudail, *Applied optics* **52**, 6350 (2013).
- [21] Z. Chen, Y. Yao, Y. Zhu, and H. Ma, *Opt. Express* **26**, 28288 (2018).
- [22] R. Meng, Z. Chen, X. Wang, Y. Liu, H. He, and H. Ma, *Appl. Opt.* **60**, 1380 (2021).
- [23] Z. Hradil, J. Řeháček, J. Fiurášek, and M. Ježek, *Quantum state estimation*, 59 (2004).
- [24] C. Macias-Romero and P. Török, *Journal of the European Optical Society - Rapid publications* **7** (2012).
- [25] R. A. Fisher *et al.*, (1920).
- [26] A. Ly, M. Marsman, J. Verhagen, R. P. Grasman, and E.-J. Wagenmakers, *Journal of Mathematical Psychology* **80**, 40 (2017).
- [27] Generally, the set of variables can be extended, for example if we work with bigger number of polarizations and if we need to define the parameters of auxiliary elements.
- [28] S. Kay, *Fundamentals Of Statistical Processing, Volume 2: Detection Theory*, Prentice-Hall signal processing series (Pearson Education, 2009).
- [29] Transmitted coefficients are not important for calibration problem in form (9), because they can be expressed as (10).
- [30] F. Goudail, *Opt. Lett.* **34**, 647 (2009).
- [31] D. Goldstein, *Polarized Light* (CRC Press, 2017).